

## **Supplementary Information**

### **Identification of peripheral neural circuits that regulate heart rate using optogenetic and viral vector strategies**

**Rajendran et al.**

<b>Power (mW)</b> (n = 6)	<b>Baseline heart rate (bpm)</b>	<b>Stimulation heart rate (bpm)</b>	<b>Δ Heart rate (%)</b>
0	355.8 ± 37.7	355.1 ± 38.0	-0.2 ± 0.2
38	365.8 ± 34.1	307.2 ± 46.1	-16.0 ± 8.7
115	353.0 ± 35.4	228.3 ± 23.7	-31.8 ± 11.0
226	379.2 ± 35.6	200.3 ± 30.0	-45.9 ± 9.7
<b>Frequency (Hz)</b> (n = 6)			
1	353.5 ± 27.2	324.6 ± 13.2	-7.2 ± 3.3
5	357.8 ± 25.7	282.4 ± 18.3	-19.7 ± 7.1
10	347.9 ± 23.0	219.7 ± 21.0	-35.2 ± 8.0
20	351.2 ± 29.0	164.5 ± 42.9	-50.0 ± 14.9
<b>Pulse width (ms)</b> (n = 6)			
1	355.6 ± 28.5	278.1 ± 23.8	-20.4 ± 8.0
2	362.1 ± 30.4	244.8 ± 25.4	-29.7 ± 10.3
10	356.6 ± 25.5	227.1 ± 21.6	-34.4 ± 8.2
<b>Atropine</b> (n = 5)			
Pre	354.9 ± 35.3	224.2 ± 25.0	-33.5 ± 11.0*
Post	333.8 ± 37.7	333.0 ± 37.9	-0.3 ± 0.2

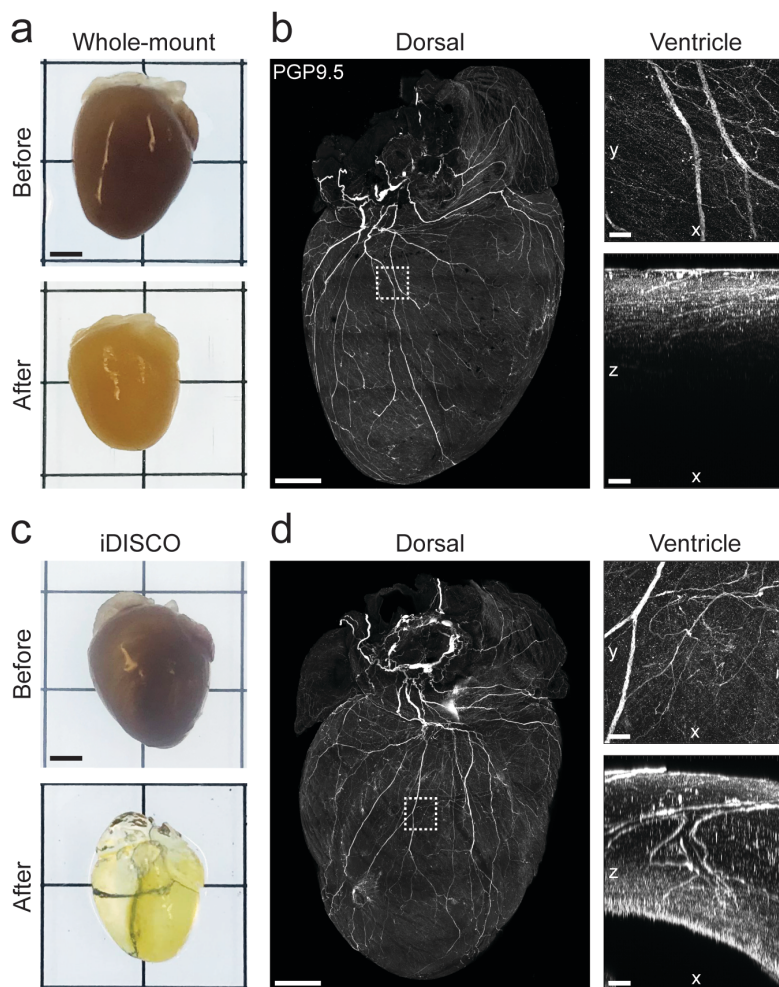
**Supplementary Table 1. Ex vivo optogenetic stimulation of cholinergic neurons in the IPV-GP.** Table corresponds to Figure 3. Dose response curves summarizing the effects of altering light pulse power, frequency, and pulse width on heart rate. Summary of the heart rate response to stimulation before versus after atropine administration ( $t_4 = 2.993$ ,  $*P = 0.0402$ ). mean ± s.e.m.; paired, two-tailed  $t$ -test.

Intact RVNS						
Frequency (Hz) (n = 8)	Optical			Electrical		
	Baseline heart rate (bpm)	Stimulation heart rate (bpm)	Δ Heart rate (%)	Baseline heart rate (bpm)	Stimulation heart rate (bpm)	Δ Heart rate (%)
1	560.7 ± 5.5	552.5 ± 5.9	-1.5 ± 0.2	594.1 ± 4.4	587.9 ± 4.5	-1.0 ± 0.2
5	561.6 ± 6.6	533.6 ± 5.3	-5.0 ± 0.3	593.4 ± 5.5	556.0 ± 8.7	-6.3 ± 0.8
10	552.0 ± 8.0	481.6 ± 8.7	-12.8 ± 0.4	590.7 ± 6.1	509.5 ± 6.3	-13.8 ± 0.6
20	558.3 ± 6.3	401.3 ± 13.0	-28.1 ± 2.2	591.6 ± 5.7	370.3 ± 32.0	-37.7 ± 5.0
<b>RVNx caudal RVNS</b>						
Frequency (Hz) (n = 3)						
1	545.8 ± 12.9	535.9 ± 13.1	-1.8 ± 0.6	564.2 ± 8.9	555.3 ± 8.0	-1.6 ± 0.5
5	550.9 ± 11.5	501.5 ± 9.2	-9.0 ± 1.0	567.7 ± 7.9	519.9 ± 13.3	-8.4 ± 1.9
10	562.2 ± 8.2	459.6 ± 19.5	-18.3 ± 2.5	568.2 ± 4.6	449.2 ± 33.0	-21.0 ± 5.7
20	549.3 ± 11.5	302.9 ± 46.0	-44.9 ± 8.1	564.2 ± 7.4	276.2 ± 47.6	-51.0 ± 8.5
<b>BVNx caudal RVNS</b>						
Frequency (Hz) (n = 3)						
1	530.0 ± 6.6	516.4 ± 5.9	-2.6 ± 0.4	558.9 ± 7.1	548.3 ± 10.6	-1.9 ± 0.7
5	534.0 ± 2.7	493.6 ± 5.7	-7.5 ± 1.5	549.8 ± 10.6	508.3 ± 28.5	-7.7 ± 3.4
10	560.6 ± 6.4	478.2 ± 16.7	-14.7 ± 2.3	546.9 ± 9.5	457.2 ± 33.8	-16.5 ± 5.1
20	545.6 ± 3.0	370.8 ± 44.5	-32.0 ± 8.3	551.5 ± 8.1	354.4 ± 69.3	-36.1 ± 11.5
<b>RVNx cranial RVNS</b>						
Frequency (Hz) (n = 5)						
1	533.4 ± 10.6	531.2 ± 10.7	-0.4 ± 0.1	569.5 ± 13.0	568.2 ± 13.5	-0.2 ± 0.2
5	539.3 ± 11.0	536.9 ± 10.5	-0.4 ± 0.2	569.6 ± 14.1	559.0 ± 19.5	-2.0 ± 1.3
10	556.6 ± 12.9	556.0 ± 12.7	-0.1 ± 0.1*	576.1 ± 10.8	539.5 ± 18.8	-6.5 ± 1.8*
20	550.1 ± 12.1	549.3 ± 11.7	-0.1 ± 0.1**	576.1 ± 11.2	519.5 ± 17.3	-9.9 ± 1.8**
<b>BVNx cranial RVNS</b>						
Frequency (Hz) (n = 5)						
1	518.5 ± 7.4	519.7 ± 8.5	0.2 ± 0.2	546.7 ± 7.5	546.9 ± 8.0	0.0 ± 0.2
5	526.1 ± 9.0	525.5 ± 9.4	-0.1 ± 0.1	545.2 ± 9.1	545.9 ± 8.9	0.1 ± 0.1
10	547.4 ± 5.9	545.5 ± 5.5	-0.3 ± 0.2	542.4 ± 8.5	539.7 ± 11.0	-0.5 ± 0.5
20	535.7 ± 6.9	534.9 ± 7.2	-0.2 ± 0.1**	545.6 ± 7.8	528.3 ± 8.7	-3.2 ± 0.4**

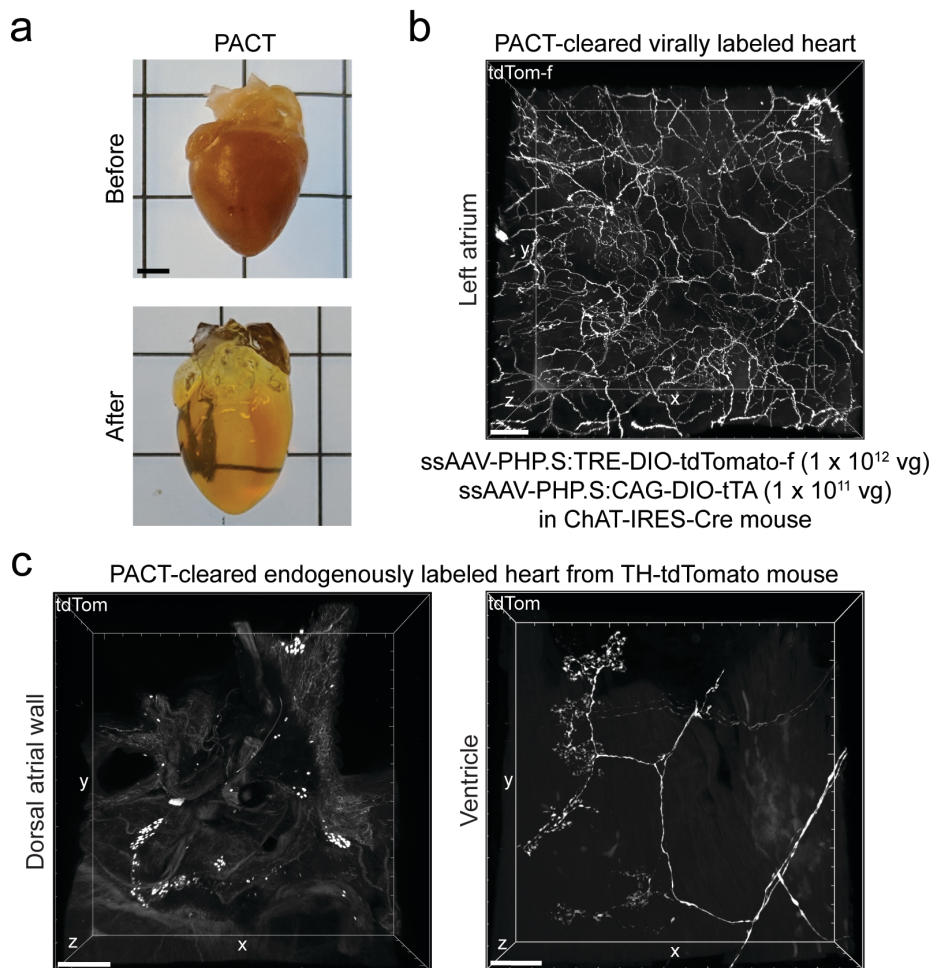
**Supplementary Table 2. *In vivo* optogenetic versus electrical stimulation of the vagus nerve.** Table corresponds to Figure 4. Frequency response curves summarizing the effects of optogenetic versus electrical stimulation of the right vagus nerve on heart rate in the intact state, of the caudal end following RVNx and BVNx, and of the cranial end following RVNx ( $t_4 = 3.576$ ,  $*P = 0.0232$  at 10 Hz;  $t_4 = 5.229$ ,  $**P = 0.0064$  at 20 Hz) and BVNx ( $t_4 = 8.588$ ,  $**P = 0.0010$  at 20 Hz). mean ± s.e.m.; paired, two-tailed *t*-test.

Frequency (Hz) (n = 7)	Baseline heart rate (bpm)	Stimulation heart rate (bpm)	$\Delta$ Heart rate (%)
1	464.8 $\pm$ 22.6	471.7 $\pm$ 22.1	1.5 $\pm$ 0.4
2	458.6 $\pm$ 21.3	476.2 $\pm$ 22.6	3.8 $\pm$ 0.6
5	459.6 $\pm$ 22.1	486.5 $\pm$ 20.6	6.1 $\pm$ 1.1
10	455.7 $\pm$ 20.8	499.5 $\pm$ 20.4	9.9 $\pm$ 1.8
20	462.4 $\pm$ 20.2	499.8 $\pm$ 18.3	8.3 $\pm$ 1.1
<b>Pulse width (ms)</b> (n = 6)			
1	469.5 $\pm$ 37.5	482.9 $\pm$ 33.8	3.4 $\pm$ 1.6
2	475.0 $\pm$ 38.8	492.0 $\pm$ 35.3	4.1 $\pm$ 1.8
5	475.3 $\pm$ 36.3	500.4 $\pm$ 33.0	5.9 $\pm$ 2.4
10	464.2 $\pm$ 32.0	499.0 $\pm$ 31.2	7.9 $\pm$ 2.2
<b>RSG versus RT2G</b> (n = 7)			
RSG	461.7 $\pm$ 24.2	504.1 $\pm$ 23.1	9.5 $\pm$ 1.8**
RT2G	486.1 $\pm$ 39.4	487.6 $\pm$ 39.3	0.3 $\pm$ 0.2
<b>Propranolol</b> (n = 4)			
Pre	471.5 $\pm$ 23.4	498.0 $\pm$ 26.0	5.6 $\pm$ 1.4*
Post	364.1 $\pm$ 20.1	364.7 $\pm$ 20.5	0.1 $\pm$ 0.1

**Supplementary Table 3. *In vivo* optogenetic stimulation of noradrenergic neurons in the RSG.** Table corresponds to Figure 6. Dose response curves summarizing the effects of altering frequency and pulse width on heart rate. Summary of the heart rate response to stimulation of the RSG versus RT2G ( $t_6 = 5.435$ , \*\* $P = 0.0016$ ). Summary of the heart rate response to RSG stimulation before versus after propranolol administration ( $t_3 = 3.951$ , \* $P = 0.0289$ ). mean  $\pm$  s.e.m.; paired, two-tailed  $t$ -test.

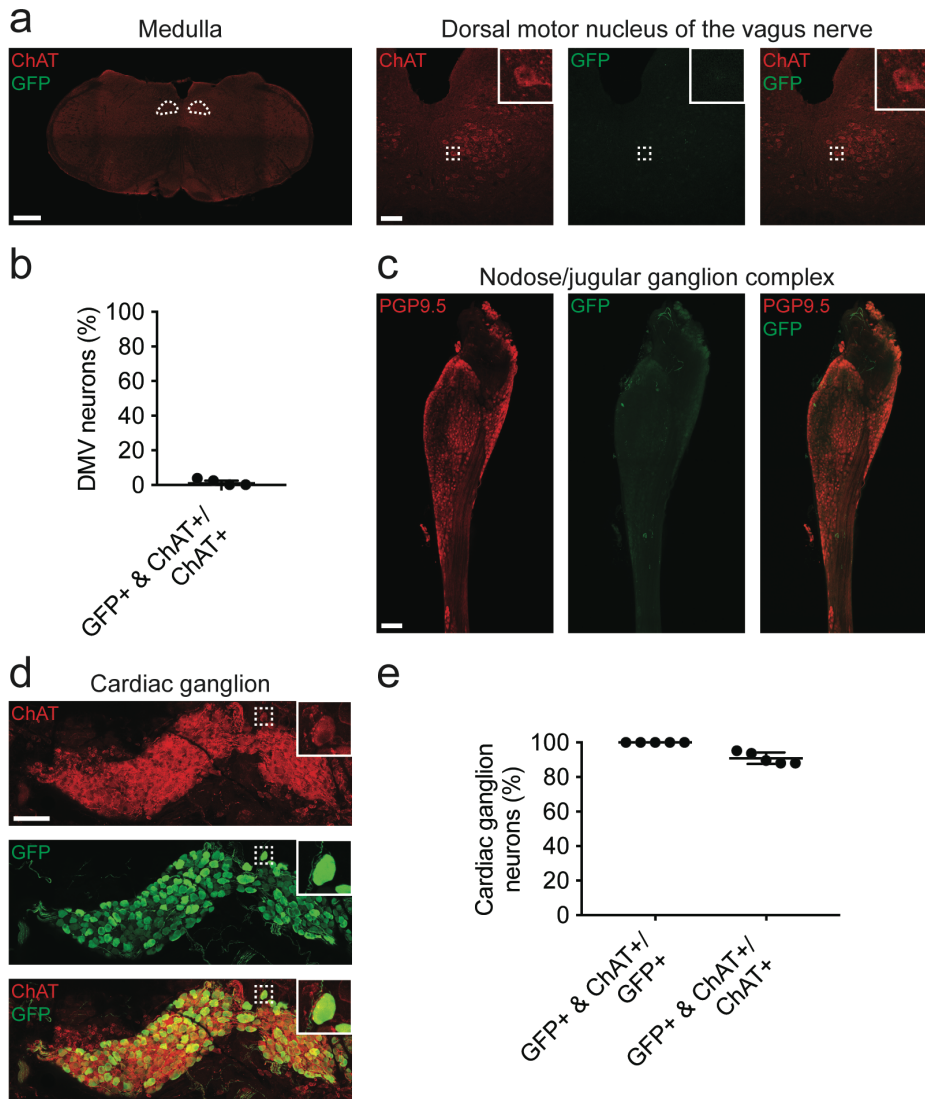


**Supplementary Figure 1. Whole-mount stained heart versus iDISCO-cleared heart.** (a) A heart before (top) and after (bottom) whole-mount staining. (b) 3D confocal projection of the dorsal side of a heart (2000  $\mu\text{m}$  z-stack) whole-mount stained with PGP9.5 (gray). Insets show a MIP image of the left ventricular wall (top right) and a 1000  $\mu\text{m}$ -thick 3D projection of the left ventricular wall (bottom right). (c) A whole heart (top) was rendered transparent (bottom) using the iDISCO protocol. (d) 3D confocal projection of the dorsal side of an iDISCO-cleared heart (2000  $\mu\text{m}$  z-stack) stained with PGP9.5 (gray). Insets show a MIP image of the left ventricular wall (top right) and a 1000  $\mu\text{m}$ -thick 3D projection of the left ventricular wall (bottom right). In contrast to whole-mount stained hearts, nerve fibers could be visualized throughout the entire thickness of myocardium in iDISCO-cleared hearts. Scale bars are 2 mm (a, c), 1 mm (b (left), d (left)), and 100  $\mu\text{m}$  (b (right), d (right)).



**Supplementary Figure 2. PACT clearing preserves fluorescence in virally and endogenously labeled hearts.** (a) Example of a whole heart (top) that was rendered transparent (bottom) using the PACT protocol. (b) ssAAV-PHP.S:TRE-DIO-tdTomato-farnesylated ( $1 \times 10^{12}$  vg) and ssAAV-PHP.S:CAG-DIO-tTA ( $1 \times 10^{11}$  vg) were systemically administered to a ChAT-IRES-Cre mouse. Four weeks later, the whole heart was cleared using the PACT protocol. A 402  $\mu\text{m}$ -thick 3D projection of the left atrium showing cholinergic nerve fibers with native tdTomato fluorescence (gray). (c) tdTomato was expressed in noradrenergic neurons by crossing transgenic TH-IRES-Cre mice with Ai14 reporter mice containing a Cre-dependent tdTomato fluorescent protein allele (TH-tdTomato). The dorsal half of a heart from a TH-tdTomato mouse was cleared using the PACT protocol. A 1000  $\mu\text{m}$ -thick 3D projection of the dorsal atrial wall showing noradrenergic neurons in cardiac ganglia with native tdTomato fluorescence (gray) (left). An 85  $\mu\text{m}$ -thick 3D projection of the ventricle showing noradrenergic nerves and nerve terminals (right). Scale bar is 2 mm (a), 100  $\mu\text{m}$  (b), 500  $\mu\text{m}$  (c, left), and 50  $\mu\text{m}$  (c, right).

ssAAV-PHP.S:CAG-DIO-eYFP ( $1 \times 10^{12}$  vg) in ChAT-IRES-Cre mice

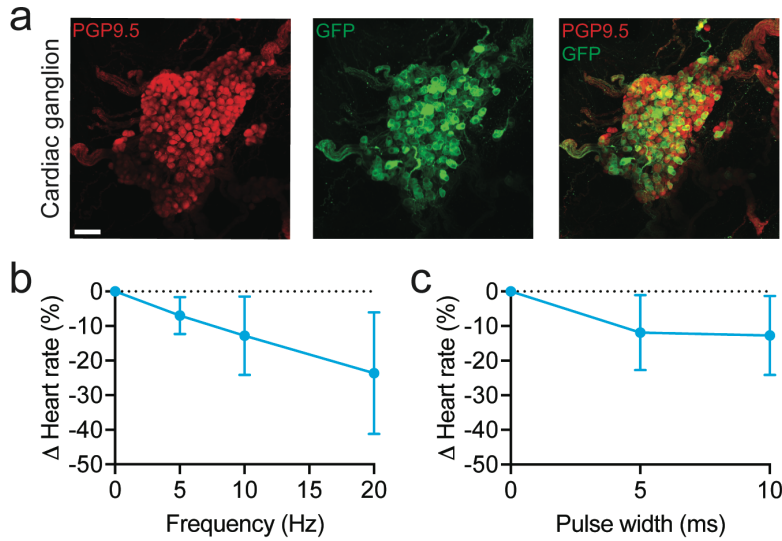


**Supplementary Figure 3. AAV-PHP.S preferentially transduces peripheral versus central cholinergic neurons.** ssAAV-PHP.S:CAG-DIO-eYFP was systemically administered to ChAT-IRES-Cre mice at  $1 \times 10^{12}$  vg per mouse. Three weeks later, eYFP fluorescence was assessed using an antibody for GFP. **(a)** Single-plane confocal images of the medulla (left) and dorsal motor nucleus of the vagus nerve (DMV) (right) whole-mount stained with ChAT (red) and GFP (green). White dashed ovals in the medulla show the location of the DMV. White dashed boxes in the DMV images indicate location of higher magnification images in white boxes. **(b)** Percentage of DMV neurons expressing GFP and ChAT over those expressing ChAT. **(c)** MIP images of the nodose/jugular ganglion complex whole-mount stained with PGP9.5 (red) and GFP (green). **(d)** MIP images of a cardiac ganglion from a heart whole-mount stained with PGP9.5 (red) and GFP (green). White dashed boxes indicate location of higher magnification images in white boxes. **(e)** Percentage of cardiac ganglion neurons expressing GFP and ChAT over those expressing GFP or ChAT, indicating specificity or efficiency of viral transduction, respectively.  $n = 4$  mice **(b)** and

5 mice (**e**); mean  $\pm$  s.e.m.. Scale bars are 500  $\mu$ m (**a** (left)), 100  $\mu$ m (**a** (right), **c**, **d** (right)), and 1 mm (**d** (left)).



ssAAV-PHP.S:CAG-DIO-ChR2-eYFP ( $1 \times 10^{12}$  vg) in ChAT-IRES-Cre mice



**Supplementary Figure 4. AAV-PHP.S for selective delivery of ChR2 to peripheral cholinergic neurons in the IPV-GP.** ssAAV-PHP.S:CAG-DIO-ChR2-eYFP was systemically administered to ChAT-IRES-Cre mice at  $1 \times 10^{12}$  vg per mouse. Experiments were performed 5 weeks post-injection. **(a)** MIP images of a cardiac ganglion from a heart whole-mount stained with PGP9.5 (red) and GFP (green). **(b, c)** Dose response curves summarizing the effects of altering stimulation frequency **(b)** and pulse width **(c)** on heart rate in Langendorff-perfused hearts.  $n = 3$  mice **(b, c)**; mean  $\pm$  s.e.m.. Scale bar is  $100 \mu\text{m}$  **(a)**.